Figure S1. The IC_{50} value of DAC in MDS-L cells was calculated via a cell growth inhibition assay. MDS, myelodysplastic syndromes; MDS-L, MDS cell line; DAC, decitabine.

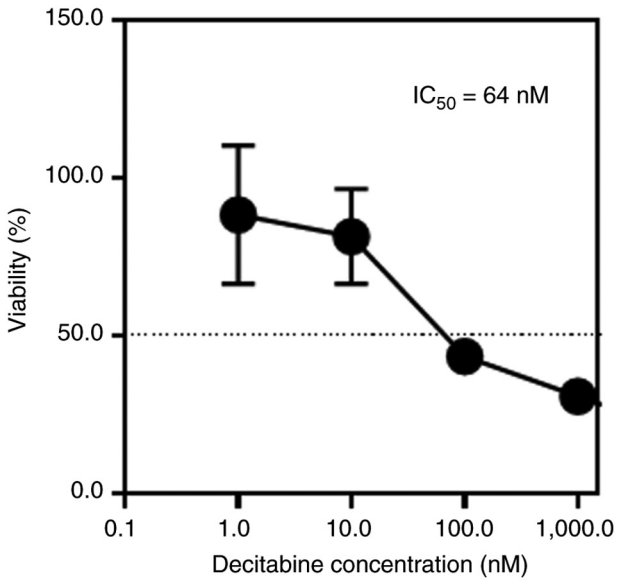

Figure S2. Immunophenotypic analysis of MDS-L cells and MDS-L-DAC cells. Flow cytometric analysis of surface makers in (A) MDS-L and (B) MDS-L-DAC cells. Cells were stained with antibodies against CD11b, CD15, CD13, CD19, CD33, CD34, CD7, CD10, HLA-DR and GP-A. Representatives dot plots are shown, and the percentages of cells in each quadrant are indicated. MDS, myelodysplastic syndromes; MDS-L, MDS cell line; DAC, decitabine; GP-A, glycophorin A; HLA-DR, MHC class II DR antigen.

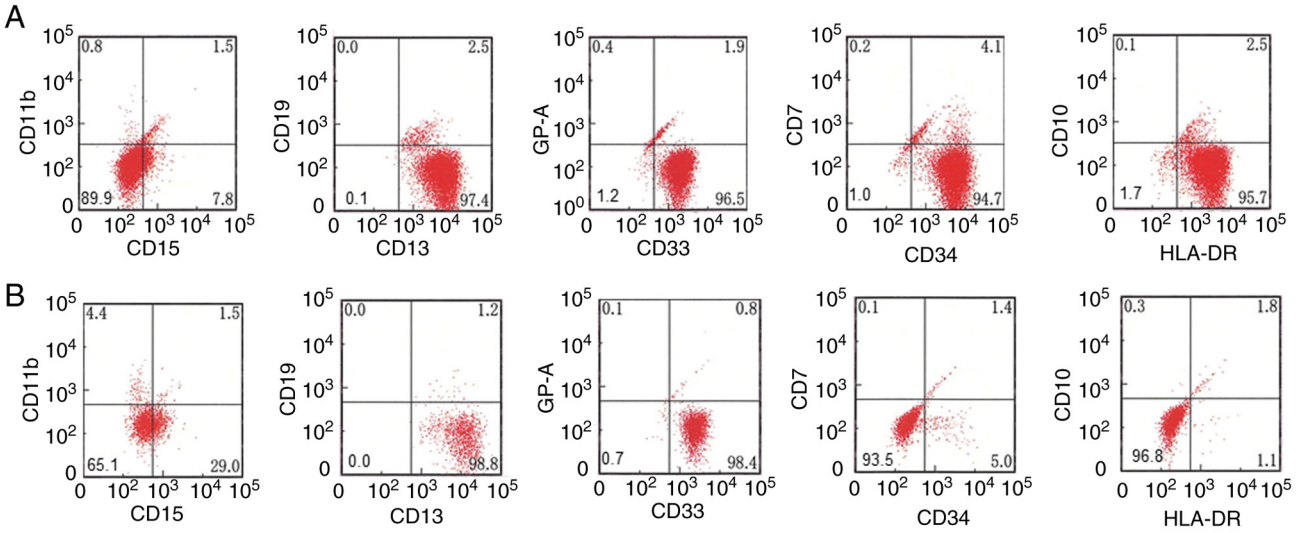

Figure S3. Chromosome analysis was performed via G-banding. (A) Representative metaphase karyotype of parental MDS-L cells showing a complex karyotype with multiple chromosomal losses and structural abnormalities. The karyotype found was 58,X,-X,-X or-Y,-2,-3,-4,der(5)t (5;?19)(q11.1;q11), -7, add(7)(q36)x2,+i(8)(q10)x2, -9,-11,-12, der(12;14)(q10;q10),-13,-14,-15, add(15)(p11.2),-17, -22,?add(22)(q11.2), der(22)t(11;22)(q13;q13),+3mar[10]. (B) Karyotype of MDS-L-DAC cells. Several structural abnormalities observed in the parental MDS-L cells were retained, while additional chromosomal alterations were detected, suggesting clonal selection. The karyotype found was 48,X,-Xor -Y,der(5)t(5;?19)(q11.1;q11), -7,add(7)(q36),i(8)(q10), der(12;14)(q10;q10),-13,-14, add(15)(p11.2),+19,+20,? add(22)(p11.2), der(22)t(11;22)(q13;q13),+4mar[5]. Arrows indicate chromosomal abnormalities. MDS, myelodysplastic syndromes; MDS-L, MDS cell line; DAC, decitabine.

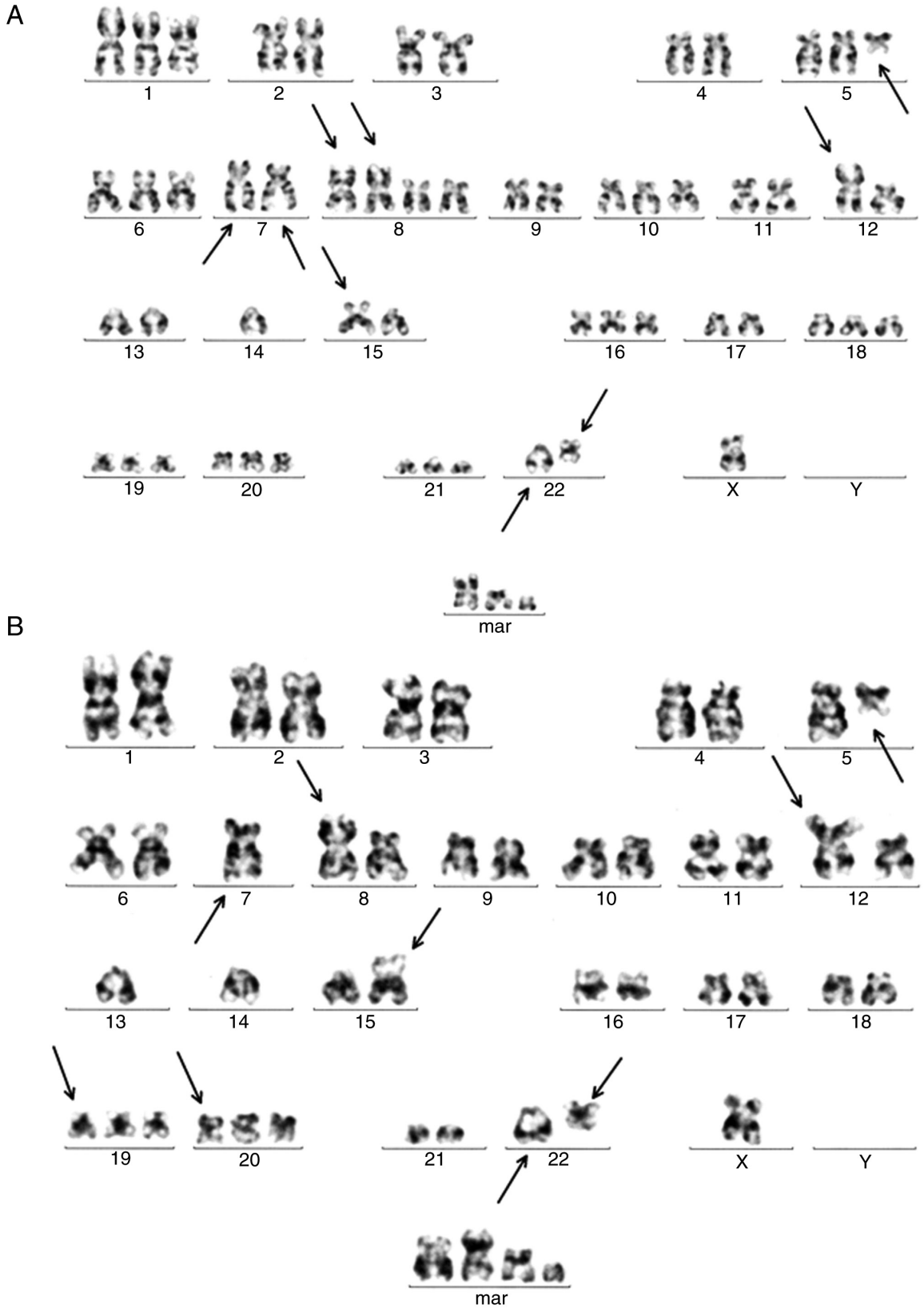

Figure S4. DNA methylation array analysis. Hierarchical clustering of differentially methylated genomic regions in MDS-L and MDS-L-DAC cells on the basis of the 100 genes and promoters with the most notable methylation changes. A gradient color scale ranging between blue (completely unmethylated) to red (completely methylated) is shown. (A) CpG site and (B) tiling. MDS, myelodysplastic syndromes; MDS-L, MDS cell line; DAC, decitabine.

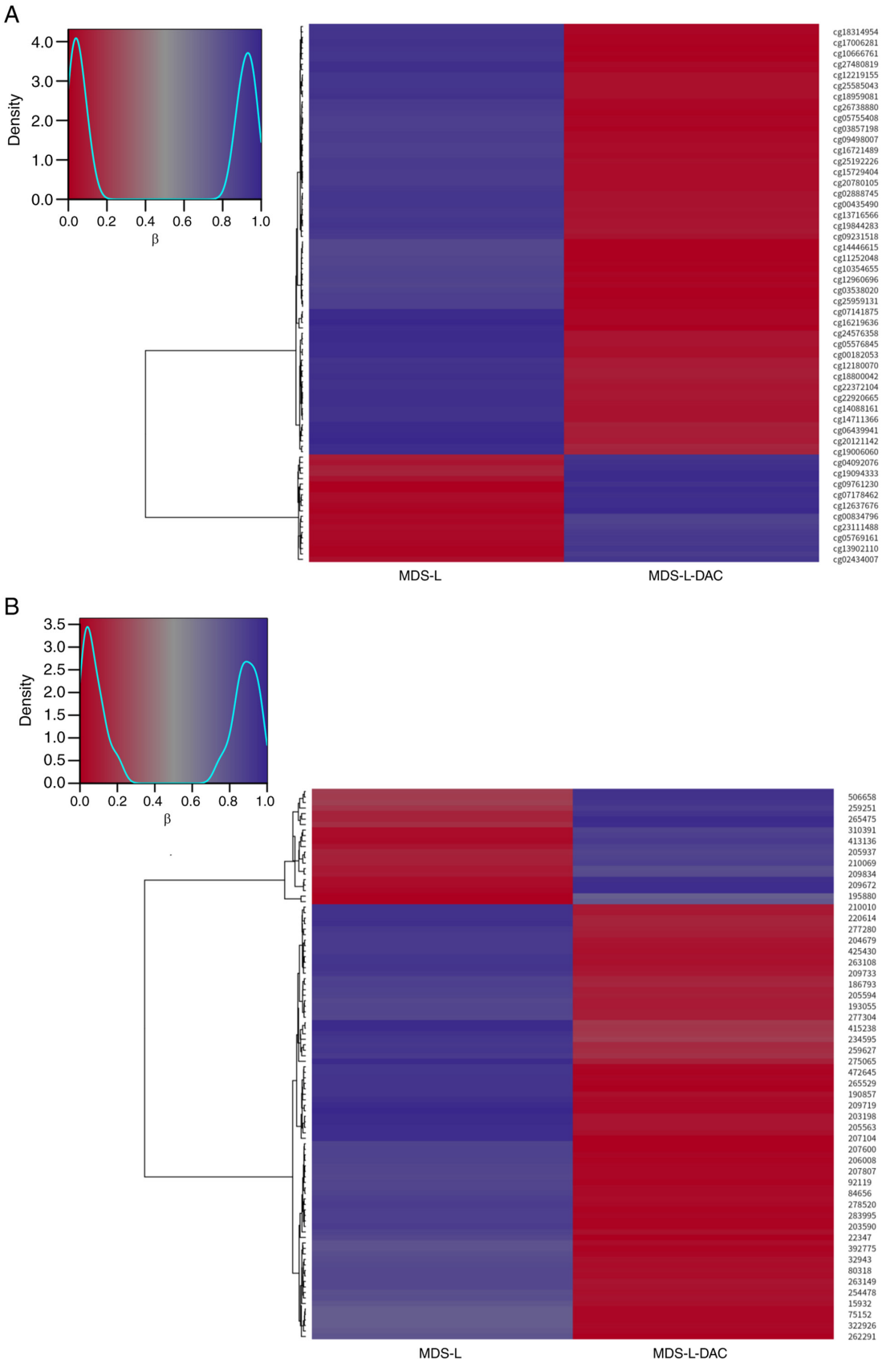

Figure S5. Flow cytometer raw data in Fig 3C. (A) Cell cycle distribution was analyzed using flow cytometry after PI staining. Representative histograms of parental MDS-L cells and MDS-L-DAC cells after long-term exposure to DAC are shown. The percentages of cells in sub-G_1, G_1, S, G_2 and M phases were calculated using flow cytometry analysis. MDS-L-DAC cells had an increased sub-G_1 population compared with parental MDS-L cells, suggesting an increased apoptosis in the MDS-L-DAC cells. (B) MDS-L cells and (C) MDS-L-DAC cells were treated with DAC (50 or 100 nM) or left untreated (control). DAC treatment increased the sub-G_1 population in both MDS-L and MDS-L-DAC cells in a concentration-dependent manner, suggesting induction of apoptosis. MDS, myelodysplastic syndromes; MDS-L, MDS cell line; DAC, decitabine.

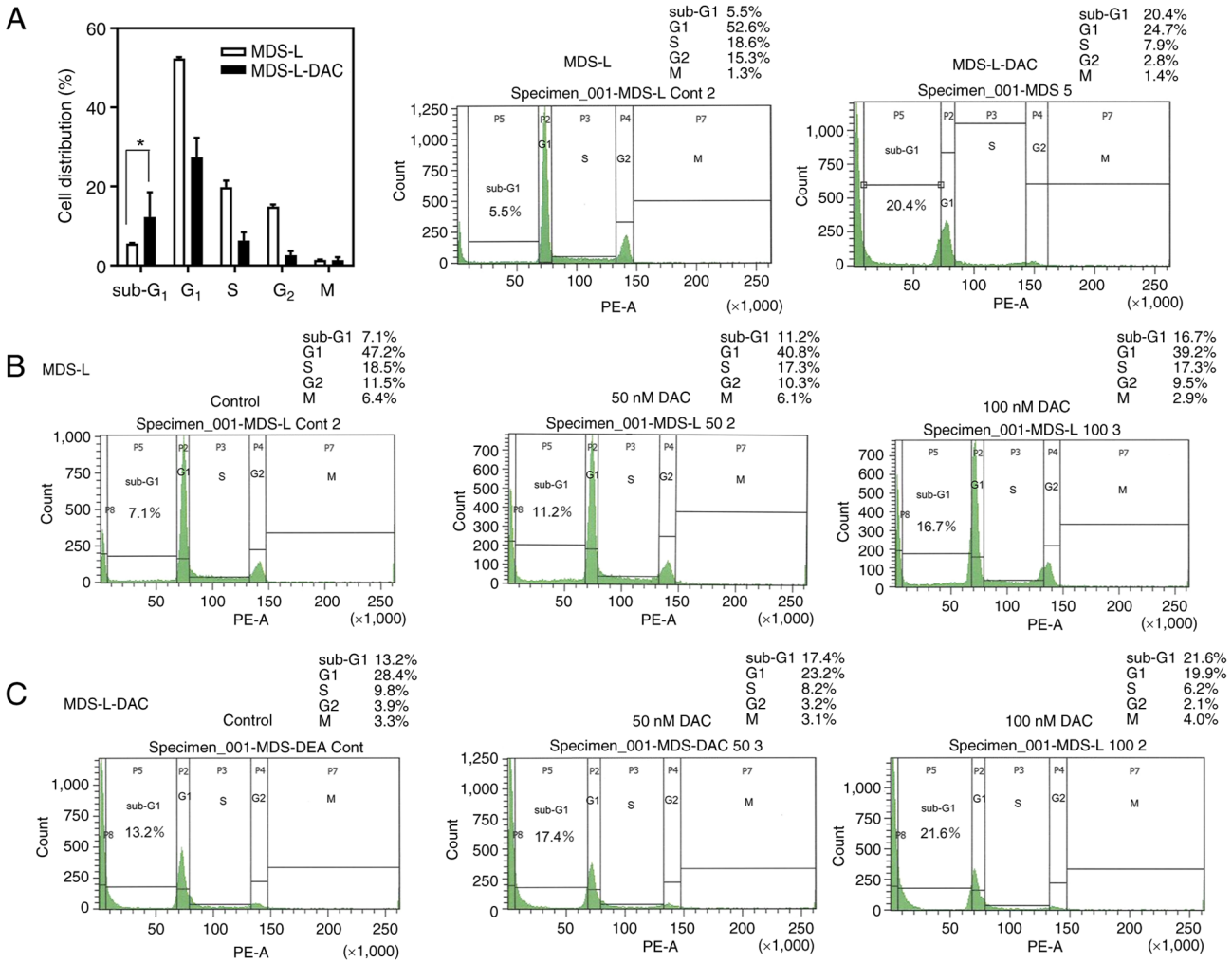

Figure S6. Flow cytometer raw data in Fig 4C. Cells were analyzed for the expression of β-catenin using flow cytometry with an Alexa Fluor 488-conjugated antibody. The left panels indicate the gating strategy based on FSC and SSC. The P1 population was selected for subsequent analysis. The right panels show representative histograms of β-catenin expression. The percentages of β-catenin-positive cells are indicated. FSC, forward scatter; SSC, side scatter; MDS, myelodysplastic syndromes; MDS-L, MDS cell line; DAC, decitabine.